

Broad absorption features in wind-dominated ultraluminous X-ray sources?

Matthew J. Middleton,¹^{*} Dominic J. Walton,² Timothy P. Roberts³ and Lucy Heil¹

¹*Astronomical Institute Anton Pannekoek, Science Park 904, NL-1098 XH, Amsterdam, the Netherlands*

²*Astronomy Department, California Institute of Technology, 1200 East California Boulevard, Pasadena, CA 91125, USA*

³*Department of Physics, University of Durham, Durham DH1 3LE, UK*

Accepted 2013 October 30. Received 2013 October 18; in original form 2013 September 12

ABSTRACT

The luminosities of ultraluminous X-ray sources (ULXs) require an exotic solution with either supercritical accretion modes on to stellar-mass black holes or subcritical accretion on to intermediate-mass black holes (IMBHs) being invoked. Discriminating between the two is non-trivial due to the present lack of a direct mass measurement. A key expectation of the supercritical mode of accretion is the presence of powerful radiatively driven winds. Here we analyse *XMM–Newton* data from NGC 5408 X-1 and NGC 6946 X-1 and find that strong soft residuals present in the X-ray spectra can be reconciled with broadened, blueshifted absorption by a partially ionized, optically thin phase of this wind. We derive initial values for the physical parameters of the wind; we also discuss other possible origins for the observed features.

Key words: accretion, accretion discs – black hole physics – X-rays: binaries.

1 INTRODUCTION

Recent studies of ultraluminous X-ray sources (ULXs: Roberts 2007; Feng & Soria 2011) in nearby galaxies have shown that, up to $\sim 3 \times 10^{39}$ erg s⁻¹, their luminosities can be robustly associated with accretion around the Eddington limit on to stellar mass ($< 100 M_{\odot}$) black holes (e.g. Middleton et al. 2012, 2013). Those with luminosities reaching $\sim 3 \times 10^{40}$ erg s⁻¹ are harder to explain, yet seem to show a trend of spectral shape with variability (Sutton, Roberts & Middleton 2013). Their behaviour appears strikingly dissimilar from the expected behaviour of sub-Eddington Galactic black hole binaries scaled up to the intermediate-mass black hole (IMBH) regime (Colbert & Mushotzky 1999, masses $> 100 M_{\odot}$), implying that they cannot *all* be IMBHs unless the characteristic properties of accretion alter dramatically beyond the expectations of simple mass scaling.

The behaviour of most bright ($3\text{--}30 \times 10^{39}$ erg s⁻¹) ULXs can plausibly be explained by stellar-mass black holes undergoing accretion in the ‘supercritical’ regime (Shakura & Sunyaev 1973). In this situation, the inflow changes at the radius where the accretion rate is locally Eddington. This drives an increase in scaleheight of the disc and optically thick winds launched radiatively from the surface (Poutanen et al. 2007; Dotan & Shaviv 2011; Ohsuga & Mineshige 2011), which are likely to be stratified due to Rayleigh–Taylor or radiative–hydrodynamic instabilities (Takeuchi, Ohsuga

& Mineshige 2013). The presence of such winds is predicted to affect the spectrum (Poutanen et al. 2007), observed luminosity (King 2009) and variability (Middleton et al. 2011), depending on the inclination angle to the observer’s line of sight and changing mass accretion rate (which we will describe fully in a forthcoming model).

Observations show that narrow atomic features in emission or absorption (namely Fe K α) must be intrinsically weak or simply not present in two of the hardest (and brightest) ULXs (Walton et al. 2012, 2013). However, in the supercritical wind model, these ‘hard ultraluminous’ ULXs are those that we view close to face-on (Sutton et al. 2013). ‘Soft ultraluminous’ ULXs, which display far higher levels of fractional variability, are thought to be viewed such that the lines of sight to the hottest inner regions are obscured by the optically thick phase of the clumpy wind (i.e. scattered out of the line of sight: Middleton et al. 2011; Middleton et al., in preparation). It is therefore these ‘soft ultraluminous’ sources in which we should expect to see atomic absorption features, the expected signatures of such outflows.

Interestingly, it has long been known that soft-spectrum ULXs can show strong residuals in their best-fitting continuum models (e.g. Stobbart, Roberts & Wilms 2006 and references therein), which have traditionally been associated with emission from collisionally heated gas in the host galaxy. However, the intrinsic luminosities in such components are very large (approaching $\sim 1 \times 10^{39}$ erg s⁻¹) and such residuals are seen in ULXs without large amounts of host galactic diffuse emission (Bachetti et al. 2013), leading some to question this identification (Middleton et al. 2011).

*E-mail: M.J.Middleton@uva.nl

Here we investigate whether absorption in the wind can account for the spectral residuals in this subset of ULXs by studying two of the brightest members of the population.

2 WIND-DOMINATED ULXS

The most variable ULXs detected are NGC 5408 X-1 (Heil, Vaughan & Roberts 2009; Middleton et al. 2011; Pasham & Strohmayer 2012) and NGC 6946 X-1 (Rao, Feng & Kaaret 2010), both with energy-integrated fractional excess variances over intra-observation time-scales of >20 per cent (and up to ~60 per cent). Both sources are also known to harbour quasi-periodic oscillations (QPOs), although determining the mass based on association with those QPOs seen in black hole binaries (BHBS; e.g. Strohmayer & Mushotzky 2009) has proven non-trivial (Middleton et al. 2011; Pasham & Strohmayer 2012).

The evolution of NGC 5408 X-1 over six deep *XMM-Newton* observations (spanning several years) has been well studied by Pasham & Strohmayer (2012), who found very little change in the X-ray spectra (although significant changes were found in the variability power spectra). The X-ray spectra show a strong soft thermal component, peaking below 1 keV with a tail of emission rolling over at 3–4 keV (such a break appears almost ubiquitously in high-quality *XMM-Newton* ULX data: Gladstone, Roberts & Done 2009, now confirmed by the Nuclear Spectroscopic Telescope Array (*NuSTAR*: Bachetti et al. 2013)). In the supercritical framework, the soft emission is from the wind (and photosphere), with the hard emission originating in a heavily distorted inner accretion disc (Poutanen et al. 2007). In addition to models describing the continuum, past studies have highlighted the need for an extra component to account for spectral residuals below 2 keV (e.g. Strohmayer & Mushotzky 2009). Should these be associated with a collisionally excited plasma (emitting as a brehmsstrahlung spectrum with overlaid emission lines) then the integrated luminosity is found to approach $\sim 1 \times 10^{39}$ erg s⁻¹. This is considerably brighter than predicted for the star-formation-related diffuse emission of the *entire* galaxy, inferred to be $\sim 3 \times 10^{37}$ erg s⁻¹ (see Dale et al. 2005; Calzetti et al. 2007; Mineo, Gilfanov & Sunyaev 2012).

Middleton et al. (2011) proposed that the large amplitudes of root-mean-square errors (rms) and trend of fractional variability with energy seen in NGC 5408 X-1 could both be explained by optically thick, clumpy material in the wind obscuring sight lines to the inner disc (e.g. Takeuchi et al. 2013). In this scenario, both the spectra and variability can be explained by supercritical accretion and are heavily influenced by the wind. NGC 6946 X-1 is not as well-studied as NGC 5408 X-1; however, Rao et al. (2010) have shown it to have both a similar X-ray spectrum and similar (in fact larger) amplitudes of rms variability on the same time-scales. Given the close association of variability and spectral behaviour in accreting sources (e.g. Muñoz-Darias, Motta & Belloni 2011), it is quite reasonable to assume both sources could be ‘wind-dominated’ ULXs.

3 SPECTRAL MODELLING

We reprocessed the six *XMM-Newton* [European Photon Imaging Camera (EPIC) MOS and PN] archival data sets of NGC 5408 X-1 (acquired from the High Energy Astrophysics Science Archive Research Center (HEASARC)¹ and the latest (proprietary) observation of NGC 6946 X-1 using the Science Analysis Software version 12

Table 1. ULX observational information.

ULX	OBSID	Obs. date	Good time (ks)
NGC 5408 X-1	0302900101	2006-01-13	85.4
	0500750101	2008-01-13	28.6
	0653380201	2010-07-17	71.8
	0653380301	2010-07-19	88.2
	0653380401	2011-01-26	73.4
NGC 6946 X-1	0653380501	2011-01-28	69.2
	0691570101	2012-10-21	81.1

Notes. Columns denote *XMM-Newton* observation identifier, date of exposure and PN spectral exposure (after accounting for background flares and dead time) for each observation studied.

(SAS 12) and up-to-date current calibration files (see Table 1 for details). We followed standard extraction procedures and filtered for soft proton flaring in the full-field, high-energy (10–15 keV) background, extracting good time intervals (GTI). As the PN has the highest response to these events, we used the PN GTI as input in extracting spectra using `XSELECT`, confirming that this removes all flares in the equivalent MOS light curves. We selected ≥ 30 arcsec radius source and background regions, with the latter selected to be on the same chip, free from sources and away from the readout direction of bright sources. The observation identifiers (OBSIDs), observation dates and useful exposures are given in Table 1. Given that the spectra of NGC 5408 X-1 do not change by a large amount at soft energies where the residuals are seen, we combined the MOS (1 and 2 separately) and PN data sets using `ADDASCASPEC`. However, as the spectrum of NGC 6946 X-1 changes markedly compared with earlier, shorter observations, we focus our analysis only on the latest, deep observation.

Initially, we proceeded to model the continuum for each source in order to identify and study the residuals. To this end we used a suitable convolved model in `XSPEC` (Arnaud 1996) representative of emission from the outer wind (`DISKBB`) and emission from the inner hot disc (`NTHCOMP`: Życki, Done & Smith 1999). The Compton component gives us the additional freedom to account for any putative Compton downscattering in the wind (Titarchuk & Shrader 2005) that may act to distort the hot disc profile, extending it to lower energies (Middleton et al., in preparation). We set the input seed photon temperature to be that of the lower temperature wind to ensure correct energy balance in the event of scattering and prevent further rollover at energies out of the bandpass (consistent with this model of accretion: Poutanen et al. 2007, recently confirmed in *NuSTAR* observations by Bachetti et al. 2013). We included absorption by neutral interstellar medium material (`TBABS`) with appropriate abundances (Wilms, Allen & McCray 2000) and lower limit set to the Galactic line-of-sight column density (NGC 5408: 6.0×10^{20} cm⁻² and NGC 6946: 2.1×10^{21} cm⁻²; Dickey & Lockman 1990). As is standard practice, we also included a constant component to account for differences between detector responses (usually <10 per cent from unity except in the case of NGC 6946 X-1 MOS1, where a dead column across the source affected the spectrum).

The results of the spectral fitting are given in Table 2 and plotted in Fig. 1. We confirm the presence of strong residuals in both NGC 5408 X-1 and NGC 6946 X-1 MOS and PN spectra. Following previous analyses of such residuals (e.g. Stobbart et al. 2006), we can model these as emission by a thermal plasma (`APEC`: Smith et al. 2001). Such models are sensitive to the heavy metal abundance; however, this is uncertain in these sources; whilst

¹ <http://heasarc.gsfc.nasa.gov/>

Table 2. XSPEC model best-fitting parameters.

TBABS*(DISKBB+NTHCOMP)								
ULX	N_{H}	kT_{d}	Γ	kT_{e}	χ^2			
5408 X-1	0.092 ± 0.003	0.193 ± 0.003	$1.65^{+0.12}_{-0.10}$	2.25 ± 0.04	2522/1663			
6946 X-1	$0.304^{+0.021}_{-0.020}$	$0.232^{+0.015}_{-0.014}$	1.96 ± 0.11	$1.63^{+0.31}_{-0.20}$	944/835			
TBABS*TBVARABS*(APEC+DISKBB+NTHCOMP)								
ULX	N_{H}	kT_{apec}	kT_{d}	Γ	kT_{e}	χ^2		
5408 X-1	$0.052^{+0.009}_{-0.008}$	1.01 ± 0.03	0.152 ± 0.008	2.36 ± 0.06	$2.09^{+0.48}_{-0.29}$	1860/1661		
5408 X-1	0.049 ± 0.004	1.02 ± 0.02	0.156 ± 0.004	2.36 ± 0.03	$2.03^{+0.21}_{-0.16}$	1894/1661		
6946 X-1	$0.028^{+0.023}_{-0.021}$	$1.14^{+0.07}_{-0.11}$	0.237 ± 0.024	$1.98^{+0.11}_{-0.12}$	$1.76^{+0.41}_{-0.25}$	788/833		
6946 X-1	$0.039^{+0.028}_{-0.025}$	$1.14^{+0.07}_{-0.09}$	$0.225^{+0.027}_{-0.025}$	$2.00^{+0.11}_{-0.12}$	$1.81^{+0.45}_{-0.27}$	785/833		
TBABS*TBVARABS*XSTAR*(DISKBB+NTHCOMP)								
ULX	N_{H}	wind N_{H}	$\log \xi$	z	kT_{d}	Γ	kT_{e}	χ^2
5408 X-1	0.028 ± 0.005	$19.8^{+23.9}_{-5.8}$	$3.44^{+0.14}_{-0.10}$	-0.12 ± 0.01	0.208 ± 0.007	2.29 ± 0.08	$1.76^{+0.36}_{-0.23}$	1997/1660
5408 X-1	0.028 ± 0.003	$6.4^{+8.3}_{-1.5}$	$3.18^{+0.05}_{-0.07}$	-0.12 ± 0.01	0.206 ± 0.004	$2.29^{+0.04}_{-0.05}$	$1.73^{+0.16}_{-0.13}$	1985/1660
6946 X-1	$0.115^{+0.014}_{-0.022}$	100.0 (>55.2)	$3.69^{+0.02}_{-0.11}$	$-0.13^{+0.01}_{-0.02}$	$0.237^{+0.019}_{-0.009}$	$2.05^{+0.12}_{-0.14}$	$1.95^{+0.57}_{-0.40}$	863/832
6946 X-1	$0.132^{+0.034}_{-0.021}$	$41.9^{+4.2}_{-1.11}$	$3.52^{+0.17}_{-0.06}$	-0.13 ± 0.01	$0.218^{+0.015}_{-0.021}$	$2.12^{+0.16}_{-0.12}$	$2.14^{+2.73}_{-0.46}$	838/832

Notes. Units of N_{H} are 10^{22} cm^{-2} and temperatures (seed photons: kT_{d} and electron plasma: kT_{e}) are quoted in keV. *Top*: Best-fitting model parameters (and 90 per cent errors) for the continuum model. *Middle*: model parameters when including thermal plasma emission with variable abundances ($0.5 Z_{\odot}$ top and Z_{\odot} bottom). *Bottom*: model parameters when including absorption in a wind with a velocity dispersion of $0.1c$ and outflow velocity of z , with $0.5 Z_{\odot}$ and Z_{\odot} (top and bottom sets of values in each case).

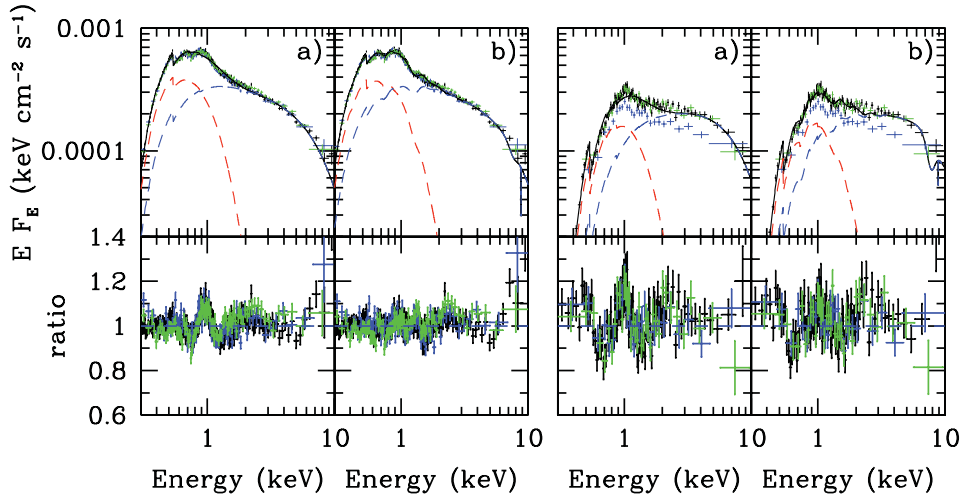


Figure 1. *Left*: (a) best-fitting continuum model (DISKBB: red dashed line; NTHCOMP: blue dashed line) to the combined data for NGC 5408 X-1 (PN: black; MOS1: blue; MOS2: green) with model parameters given in Table 2. Residuals to the fit are shown in the panel below and clearly show an excess at 1 keV. (b) Best-fitting model incorporating a partially ionized, optically thin wind (see Table 2 for best-fitting parameters), in this case with $0.5 Z_{\odot}$. The residuals have been substantially reduced. *Right*: as for left panels, with data of NGC 6946 X-1 and best-fitting models. Note that the MOS1 data are lower due to the source region being affected by a dead column.

observations of the NGC 5408 X-1 environment (Mendes de Oliveira et al. 2006) imply subsolar abundance, X-ray spectral fitting (Winter, Mushotzky & Reynolds 2007) measures abundances closer to solar (there are no equivalent constraints for NGC 6946 X-1, although the galactic metallicity is \sim solar: Moustakas et al. 2010). To account for these uncertainties, we tested abundances set at $0.5 Z_{\odot}$ and Z_{\odot} . In order to be fully consistent, we included a second, variable abundance absorption column (TBVARABS) where we fixed the heavy metals (above He) to the abundance in the APEC component, redshift to zero and the column density of the TBABS component to its Galactic value. The model fitting (Table 2) gives

thermal plasma luminosities of $3.9\text{--}5.3$ (NGC 5408 X-1) and $2.8\text{--}5.6 \times 10^{38} \text{ erg s}^{-1}$ (NGC 6946 X-1) for Z_{\odot} and $0.5 Z_{\odot}$, far greater than the inferred diffuse luminosity of either galaxy (Dale et al. 2005; Mineo et al. 2012) given the ratio of the extraction region area to the projected galaxy area: $\sim 1 \times 10^{27} \text{ erg s}^{-1}$.

Should the residuals instead be the result of absorption in the line of sight by an outflowing, optically thin phase of a supercritical wind, then by making some basic assumptions we can model these features using a table made with XSTAR2XSPEC (Kallman & Bautista 2001). Based on the simulations of Takeuchi et al. (2013), we may expect wind element sizes of $\sim 10 R_s$. If we (naively)

assume that the column density of winds in BHBs when extremely bright ($\sim 10^{24} \text{ cm}^{-2}$, e.g. Revnivtsev et al. 2002) is of the order of what we might expect to see in ULXs, then this places an upper limit on the particle density of 10^{17} cm^{-3} . As this upper limit gives a Thompson scattering optical depth ≤ 1 at these columns, we are satisfied that this is an appropriate, albeit crude, value to use in this initial modelling. We used the best-fitting de-absorbed model to the continuum to provide the input ionizing flux and produced four grids per source, stepping between $\log \xi$ of 3 and 4 in five linear steps and column densities of 1×10^{22} and 1×10^{24} (limited so that the optical depth is less than unity) in eight logarithmic steps. As we do not know the velocity dispersion a priori, we set the turbulent velocity (as a proxy for velocity dispersion) in the wind to be $0.01c$ and $0.1c$ (the predicted outflow velocity is an obvious upper limit: Takeuchi et al. 2013) and produced grids at $0.5Z_{\odot}$ and Z_{\odot} . In all grids we set the covering fraction to be unity as a limiting case. Fitting the resulting grids with the continuum (again using TBVARABS with matching abundances) in XSPEC, we find the larger velocity dispersion of $0.1c$ to be statistically favoured (by $\Delta\chi^2 > 50$). Whilst including smeared absorption yields a highly significant improvement in $\Delta\chi^2$ from the continuum model (Table 2), this is evidently not as great as that obtained by including a thermal plasma (in both cases the fit quality remains poor for NGC 5408 X-1). However, we attribute this (and the spectral residuals in Fig. 1) to the simplicity of our model; it only accounts for a single phase of the absorber (we do not fit multiple grids to avoid compounding caveats), yet there are likely to be multiple phases of differing densities (Takeuchi et al. 2013).

At the relatively high ionization states inferred for the wind, H and He have no effective opacity and do not affect the shape of the spectrum. As a result, the different abundances in the grids are somewhat balanced by column density and ionization state. Although we cannot be certain of the correct abundance at this time, we can use both best-fitting models (the parameters of which are given in Table 2) to determine the likely range of parameters for the wind. Given the particle density and range of $\log \xi$, we can obtain a rough estimate for the location of the material relative to the central illuminating source. This explicitly assumes that the wind is exposed to the same de-absorbed, 0.3–10 keV X-ray luminosities that we observe: 7.7 and $7.6 \times 10^{39} \text{ erg s}^{-1}$ for NGC 5408 X-1 and NGC 6946 X-1 respectively (determined by integrating below the continuum model in Table 2). Following Tarter, Tucker & Salpeter (1969): $R \geq \sqrt{L_x / (\xi n_e)}$, we find $R > 5200R_g$ and $> 3400R_g$ for a $10\text{-}M_{\odot}$ BH and for each source respectively (with the aforementioned caveats).

Using equation (1) of Ponti et al. (2012), we can obtain a crude estimate for the mass outflow rate in this phase of the wind:

$$\dot{M}_w = 4\pi m_p v_{\text{out}} \frac{L_x}{\xi} \frac{\Omega}{4\pi r}, \quad (1)$$

where Ω is the covering fraction of the wind, m_p is the proton mass and v_{out} is the outflow velocity. We can also estimate the mass inflow rate through the inner radius using the relations of Poutanen et al. (2007):

$$\dot{M}_o = M_{\text{BH}}^{-1/2} \left(\frac{1.5 f_c}{T_{c,\text{sph}}[\text{keV}]} \right)^2, \quad (2)$$

$$\dot{M}_{\text{in}} \approx \frac{\dot{M}_o(1-a)}{1-a \left(\frac{2}{5} \dot{M}_o \right)^{-1/2}}, \quad (3)$$

where \dot{M}_o is the local mass accretion rate (in Eddington units), $T_{c,\text{sph}}$ is the temperature at the wind spherization radius, R_{sph} , f_c (the colour temperature correction due to Compton scattering) is assumed to be 1.7 (Poutanen et al. 2007), $a = \epsilon_w(0.83 - 0.25\epsilon_w)$ and ϵ_w is the fraction of radiative energy used to launch the wind. From the spectral fits, we obtain $T_{c,\text{sph}}$ (kT_d). If we then assume the unphysical but limiting value of $\epsilon_w = 1$ (assuming maximal energy launches the wind and thus the largest mass loss) and use the results of the model fitting, we obtain an upper limit on the mass outflow to inflow (to the BH) ratio of < 1.1 and < 0.7 for NGC 5408 X-1 and NGC 6946 X-1, respectively. In deriving the ratio, we have assumed an accretion efficiency of 0.08 (standard for a Schwarzschild BH) with values differing mostly due to the lower limit on $\log \xi$ for NGC 5408 X-1. There are naturally several caveats: e.g. this only accounts for this partially ionized phase of the wind and the covering fraction was set at unity (though Walton et al. 2013 rule this out). We will explore these caveats in detail in a future work.

4 DISCUSSION AND CONCLUSIONS

Given the bright nature of ULXs, it is natural to assign their properties to an exotic accretion scenario, either the presence of IMBHs or supercritical accretion modes on to stellar mass BHs. Assuming a common scaling of BH accretion physics (spectrum, variability, outflows, etc.), the predictions for IMBHs are clear. At the inferred Eddington ratios we would expect generally hard spectra (rolling over well out of the *XMM-Newton* bandpass), with large amounts of fractional variability (e.g. Muñoz-Darias et al. 2011). Whilst the amount of ‘fast’ variability in some ULXs seems to be an adequate match (though we caution that the QPOs do not yet provide a strong lever arm for identification), e.g. Caballero-García, Belloni & Wolter 2013, the spectra and behaviour seem to depart from expectation (see Gladstone et al. 2009; Sutton et al. 2013; Bachetti et al. 2013; Middleton et al., in preparation). One thing is clear: at these accretion rates we do not expect IMBHs to be powering substantial winds (assuming scaling of accretion properties holds at these intermediate mass ranges). Conversely, if we infer the presence of accretion on to stellar mass BHs we *must* invoke supercritical accretion and winds if we are to explain bright ($3 < L_x < 30 \times 10^{39} \text{ erg s}^{-1}$) ULXs and their coupled spectra and variability (Sutton et al. 2013).

We can explain the large amounts of variability seen in some soft ULXs if they are ‘wind-dominated’, i.e. viewed at moderate inclinations, into the cone of the wind expected to accompany supercritical accretion (Middleton et al. 2011). In the cases of the two best observed of these, NGC 5408 X-1 and NGC 6946 X-1, strong residuals are seen at soft energies. Although these can be described by thermal plasma emission, the luminosities appear improbably large for host galactic diffuse emission at the position of the source. If we instead associate these with collisionally excited circumequatorial material (perhaps from earlier wind epochs), then we could generate the observed luminosities (Roberts et al. 2004). Such emission should be isotropic, yet we appear to see these residuals predominantly in sources with soft spectra (and generally large amounts of fractional variability at high energies), e.g. the ‘ULX dipper’, NGC 55 ULX1 (Stobbart, Roberts & Warwick 2004). Conversely we note the overall lack of strong variability and residuals in those brightest and hardest ULXs thought to be viewed face-on (Sutton et al. 2013), which are also constrained to show only very weak (or no) narrow iron features (Walton et al. 2012; 2013). This could be a remarkable coincidence, or else line-of-sight/inclination effects are an obvious solution (the lack of narrow emission in the hardest sources will be addressed in future work).

Our analysis has shown that absorption by an optically thin plasma, outflowing into the line of sight and ionized by the central source, can broadly account for the residuals. We can reconcile this within the model of supercritical accretion where, at larger distances, the initially optically thick material in the wind disperses in the direction of the outflow (as the wind elements themselves are not in hydrostatic equilibrium) and becomes optically thin. Although the density of material drops, should the combination of distance from the ionizing source and self-shielding (by the inner wind) allow the ionization of the material to drop, we should see the effect of absorption by ionized species of abundant elements. Due to the velocity dispersion in the outflow, we would expect the lines to appear smeared and blueshifted when looking into the outflowing path of the wind. In this way, they are effectively analogous to the lines seen in broad absorption line quasi-stellar objects (BALQSOs) at lower energies. Admittedly, the model we have used is only simple (as can be seen from the moderately poor fit statistics) and lacks an accurate physical description of the outflow, radiative transfer and effect of self-shielding. However, this first step, whilst tentative, is still enlightening as it allows us to place initial constraints on certain physical parameters of the wind (which will be reviewed and updated as the models to describe the spectral imprint of these winds develop). Based on the results of our modelling, we suggest that the optically thin wind is $>1000R_g$ from the ionizing source and may carry a large fraction of matter and energy from the accretion flow. We argue that this identification is the most likely and is the natural expectation of supercritical accretion. However, while this interpretation is the natural expectation for the supercritical regime, we are unlikely to be able to distinguish conclusively between this and other plausible explanations until the advent of missions carrying high-throughput, high-energy resolution instrumentation, e.g. *Astro-H* (Takahashi et al. 2010).

ACKNOWLEDGEMENTS

The authors thank Tim Kallmann for insights into the use of XSTAR2XSPEC. MJM acknowledges support via a Marie Curie FP7 Postdoctoral scholarship. TPR was funded as part of the STFC consolidated grant ST/K000861/1. This work is based on observations obtained with *XMM-Newton*, an ESA science mission with instruments and contributions directly funded by ESA Member States and NASA. We thank the anonymous referee for useful suggestions.

REFERENCES

Arnaud K. A., 1996, in Jacoby G. H., Barnes J., eds, ASP Conf. Ser. Vol. 101, *Astronomical Data Analysis Software and Systems V*. Astron. Soc. Pac., San Francisco, p. 17
 Bachetti M. et al., 2013, *ApJ*, 778, 163
 Caballero-García M. D., Belloni T. M., Wolter A., 2013, *MNRAS*, 435, 2665

Calzetti D. et al., 2007, *ApJ*, 666, 870
 Colbert E. J. M., Mushotzky R. F., 1999, *ApJ*, 519, 89
 Dale D. A. et al., 2005, *ApJ*, 633, 857
 Dickey J. M., Lockman F. J., 1990, *ARA&A*, 28, 215
 Dotan C., Shaviv N. J., 2011, *MNRAS*, 413, 1623
 Feng H., Soria R., 2011, *New Astron. Rev.*, 55, 166
 Gladstone J. C., Roberts T. P., Done C., 2009, *MNRAS*, 397, 1836
 Heil L. M., Vaughan S., Roberts T. P., 2009, *MNRAS*, 397, 1061
 Kallman T., Bautista M., 2001, *ApJS*, 133, 221
 King A. R., 2009, *MNRAS*, 393, L41
 Mendes de Oliveira C. L., Temporin S., Cypriano E. S., Plana H., Amram P., Sodré L., Jr, Balkowski C., 2006, *AJ*, 132, 570
 Middleton M. J., Roberts T. P., Done C., Jackson F. E., 2011, *MNRAS*, 411, 644
 Middleton M. J., Sutton A. D., Roberts T. P., Jackson F. E., Done C., 2012, *MNRAS*, 420, 2969
 Middleton M. J. et al., 2013, *Nature*, 493, 187
 Mineo S., Gilfanov M., Sunyaev R., 2012, *MNRAS*, 426, 1870
 Moustakas J., Kennicutt R. C., Jr, Tremonti C. A., Dale D. A., Smith J.-D. T., Calzetti D., 2010, *ApJS*, 190, 233
 Muñoz-Darias T., Motta S., Belloni T. M., 2011, *MNRAS*, 410, 679
 Ohsuga K., Mineshige S., 2011, *ApJ*, 736, 2
 Pasham D., Strohmayer T. E., 2012, *ApJ*, 753, 139
 Ponti G., Fender R. P., Begelman M. C., Dunn R. J. H., Neilsen J., Coriat M., 2012, *MNRAS*, 422, L11
 Poutanen J., Lipunova G., Fabrika S., Butkevich A. G., Abolmasov P., 2007, *MNRAS*, 377, 1187
 Rao F., Feng H., Kaaret P., 2010, *ApJ*, 722, 620
 Revnivtsev M., Gilfanov M., Churazov E., Sunyaev R., 2002, *A&A*, 391, 1013
 Roberts T. P., 2007, *Ap&SS*, 311, 203
 Roberts T. P., Warwick R. S., Ward M. J., Goad M. R., 2004, *MNRAS*, 349, 1193
 Shakura N. I., Sunyaev R. A., 1973, *A&A*, 24, 337
 Smith R. K., Brickhouse N. S., Liedahl D. A., Raymond J. C., 2001, *ApJ*, 556, L91
 Stobbart A.-M., Roberts T. P., Warwick R. S., 2004, *MNRAS*, 351, 1063
 Stobbart A.-M., Roberts T. P., Wilms J., 2006, *MNRAS*, 368, 397
 Strohmayer T. E., Mushotzky R. F., 2009, *ApJ*, 703, 1386
 Sutton A. D., Roberts T. P., Middleton M. J., 2013, *MNRAS*, 435, 1758
 Takahashi T. et al., 2010, *SPIE*, 7732
 Takeuchi S., Ohsuga K., Mineshige S., 2013, *PASJ*, 65, 88
 Tarter C. B., Tucker W. H., Salpeter E. E., 1969, *ApJ*, 156, 943
 Titarchuk L., Shrader C., 2005, *ApJ*, 623, 362
 Walton D. J., Miller J. M., Reis R. C., Fabian A. C., 2012, *MNRAS*, 426, 473
 Walton D. J., Miller J. M., Harrison F. A., Fabian A. C., Roberts T. P., Middleton M. J., Reis R. C., 2013, *ApJ*, 773, L9
 Wilms J., Allen A., McCray R., 2000, *ApJ*, 542, 914
 Winter L. M., Mushotzky R. F., Reynolds C. S., 2007, *ApJ*, 655, 163
 Życki P. T., Done C., Smith D. A., 1999, *MNRAS*, 309, 561

This paper has been typeset from a $\text{\TeX}/\text{\LaTeX}$ file prepared by the author.